IJE TRANSACTIONS A: Basics Vol. 34, No. 04, (April 2021) 843-853

International Journal of Engineering

Journal Homepage: www.ije.ir

Proposing a New Image Watermarking Method Using Shearlet Transform and Whale Optimization Algorithm

M. Saadati[a], J. Vahidi*[b], V. Seydi[a], P. Sheikholharam Mashhadi[a]

[a] Department of Computer Engineering, Artificial Intelligence, South Tehran Branch, Islamic Azad University, Tehran, Iran
[b] Department of Applied Mathematics, Iran University of Science and Technology, Tehran, Iran

PAPER INFO

Paper history:
Received 14 December 2020
Received in revised form 10 February 2021
Accepted 16 February 2021

Keywords:
Shearlet Transform
Whale Optimization Algorithm
Singular Value Decomposition
Image Watermarking

ABSTRACT

Digital watermarking is a method for data hiding that ensures the security of multimedia data. The watermark can be a digital image or data stored within digital content. The Shearlet transform, a multi-resolution and multi-directional conversion, can be used for watermarking in digital images. Due to its superior features, this conversion can increase the efficiency of applications such as watermarking of images. In this paper, Shearlet and the Singular Value Decomposition (SVD) transforms are used with the Whale optimization algorithm to obtain the most appropriate scaling factor in the watermark extraction step after applying different types of image processing attacks. Shearlet transform has more transparency than traditional converts. The SVD transform also increases the robustness of watermarking operations. The results of different experiments show that the new method presented in this paper, in terms of robustness and imperceptibility compared to the evaluated methods, performs better than most image processing attacks.

doi: *10.5829/ije.2021.34.04a.10*

1. INTRODUCTION

In recent years, computer networks' dramatic growth has facilitated multimedia data dissemination such as images, videos, and audios. Multimedia data can be easily copied and published without the owner's consent. There are different ways to prevent unauthorized disseminations, one of which is digital watermarking. A watermark can be a logo, digital signature, etc., inserted in the host image. Therefore, the image owner can prove the suspicious image from the watermarking image via retrieving the watermark. The main purpose of digital watermarking is embedding the watermark information invisible and usually resistant in digital content [1]. In recent decades many new techniques and concepts have been introduced in the field of image watermarking. They have been used as a tool for detecting changes in digital images as well as image authentication.

A digital watermark is a visible or invisible identification code. It may contain some information about the legal recipient or author of the original data and copyright laws in the form of textual or visual data stored. This digital watermark can be identified or extracted and later used to claim real ownership of the data. The lack of a watermark in the previously watermarking image means the digital data content has changed.

Discrete Cosine Transforms (DCT) [2-4], Discrete Wavelet Transforms (DWT) [5-8], and the Singular Value Decomposition (SVD) Transform [5-14] are the most commonly used frequency domain transformations for watermarking. According to the papers, some hybrid watermarking techniques using the SVD transform can also be mentioned [4-11, 15-17]. Several watermarking studies that use optimization and evolutionary algorithms are Genetic Algorithm (GA) [18-20], Particle Swarm Optimization (PSO) Algorithm [21, 22], and Bee Colony (BC) Algorithm [2, 10, 15, 23] and Wolf Optimization Algorithm [24]. Abdelhakim et al. proposed a resistant watermarking method using the DCT conversion and bee colony algorithm [2]. Seardean et al. proposed a watermarking method in the Wavelet transform domain [24]. Mishra et al. developed a resistant watermarking

*Corresponding Author Institutional Email: jvahidi@iust.ac.ir (J. Vahidi)

Please cite this article as: M. Saadati, J. Vahidi, V. Seydi, P. Sheikholharam Mashhadi, Proposing a New Image Watermarking Method Using Shearlet Transform and Whale Optimization Algorithm , International Journal of Engineering, Transactions A: Basics Vol. 34, No. 04, (2021) 843-853

method in the DWT-SVD transform domain [7]. Ali et al. used the Differential Evolution (DE) algorithm to find the appropriate scaling factor in the DWT-SVD algorithm [5]. Block-based watermarking was suggested by Makbol et al. using Wavelet transform and the SVD transform [8]. Fazli and Moeini developed a resistant watermarking method utilizing a fusion of Wavelet transform and DCT, and the SVD transform [17]. Zhao et al. proposed a new approach using Shearlet transform and the entropy rate [25]. Xiang-yang et al. proposed a watermarking method that employs watermarking in the sub-band with the highest amount of energy [26].

The rest of the paper is organized as follows. In Section 2, we review the Materials and Methods. Section 3 presents the proposed method in this paper. Section 4 illustrates the evaluation of results. Section 5 shows the result of simulations and experiments. Finally, Section 6 concludes this paper.

2. MATERIALS AND METHODS

2. 1. Classification of Digital Watermarking Methods Watermark embedding techniques can be divided into two main groups. Below is a brief description of the features of these groups.

In spatial domain techniques, the watermark is added directly to the original image by changing its pixel values. These algorithms are simple, fast, and have a high embedded capacity [27]. These techniques are susceptible to changes that can damage the watermark [28, 29]. Spatial-based techniques' disadvantages are more than their advantages that cannot withstand many attacks, such as added noise and compression methods [30]. Techniques for this class include Least Significant Bit (LSB) [31], Local Binary Pattern (LBP) [32], and Histogram modification [33].

Compared to spatial domain methods, in transform domain techniques, the goal is to incorporate watermarking into image coefficients. The host image is first transmitted from the spatial domain to the transform domain with a reversible conversion and after inserting the tokens with a suitable embedding algorithm. An important issue in this area is to choose the best place for watermarking to avoid image distortion. The transform field is resistant to change, attack and the watermark can be invisibly embedded in the image [28, 29]. Techniques of this method include DCT [34], Discrete Fourier Transform (DFT) [35], and DWT [6].

2. 2. Shearlet Transform A useful feature of Wavelets is their ability to find the image features in horizontal, vertical, and diagonal directions. However, Wavelets are not capable of identifying image-oriented features in other directions because of isotropic bases. To solve this problem and find features in different directions, we can use other multi-scale directional transformations. A qualified feature of these transformations in watermarking operations is that we can embed the watermark in differently oriented sub-bands of image. These multi-scale and multi-resolution transformations include Wavelet, Contourlet, and Shearlet transform. The Contourlets have bases made of a combination of directional and multi-scale filter banks [36].

In 2005, a new approach was proposed by Labate et al. [37], called Shearlet, which obtained a near-optimal approximation [38]. The Shearlet display has been introduced as a multi-directional Wavelet method that provides almost optimal features in recent years. This new representation is based on a resistant and simple mathematical framework that provides a flexible tool for geometric representation of multi-dimensional data and is also more natural for implementation. The Shearlet method is also related to multi-resolution analysis [36]. Figure 1 shows the frequency domain of the Shearlet transform [39].

The continuous 2D Shearlet transform (Shearlet's mother) in $\psi \in L^2(R^2)$ space is defined as Equation (1):

$$\begin{aligned}\psi_{a,s,t}(x) &= a^{-3/4}\psi(A_a^{-1}S_s^{-1}(x-t)) \\ &= a^{-3/4}\psi\left(\begin{pmatrix}\frac{1}{a} & \frac{-s}{a}\\ 0 & \frac{1}{\sqrt{a}}\end{pmatrix}(x-t)\right), a>R^+, s\in R, t\in R^2\}\end{aligned} \quad (1)$$

where ψ is called the generator function, A and S are 2x2 invertible matrices. A is the parabolic scaling matrices, and S is the Shear matrices [37], as:

$$A_a = \begin{bmatrix} a & 0 \\ 0 & a^{1/2} \end{bmatrix}, \quad S_s = \begin{bmatrix} 1 & s \\ 0 & 1 \end{bmatrix} \quad (2)$$

Applying the Fourier transform to the continuous Shearlet transform is obtained using Equation (3):

$$SH_\psi(f) = \langle f, \psi_{a,s,t} \rangle \quad (3)$$

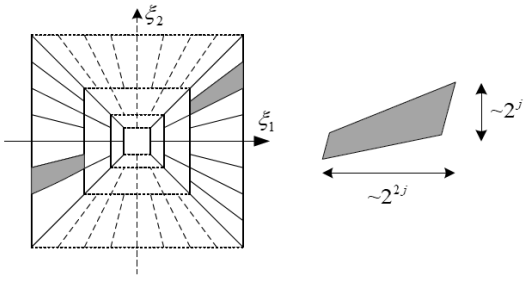

Figure 1. The frequency space of the Shearlet transform [39]

The digital image is considered as sampled functions on the network with

$$\{(\frac{m_1}{M},\frac{m_2}{N}):(m_1,m_2)\in I\}$$

$I=\{(m_1,m_2):m_1=\circ,...,M-1,m_2=\circ,...,N-1\}\cdot$

We have acquired a discrete Shearlet by discretizing the parameters *a*, *s*, and *t*. Suppose $j=\left\lfloor \frac{1}{2}\log_{\circ} N \right\rfloor$ is the number of levels taken into account. A discrete Shearlet transform must be obtained. The scale, shear, and transfer parameters are discretized :

$a_j=2^{-2j}=\frac{1}{4^j} \qquad j=\circ,...,j_\circ-1$

$s_{j,k}=k2^{-j} \qquad 2^{-j}\le k\le 2^j$

$t_m=(\frac{m_1}{M},\frac{m_2}{N}) \qquad m\in I$

With these symbols, discrete Shearlets are defined as Equation (4):

$$\psi_{j,k,m}(x)=\psi(A_{a_j}^{-1}S_{s_{j,k}}^{-1}(x-t_m)) \tag{4}$$

The discrete Shearlet transform is defined as Equation (5):

$$SH_\psi(f)=\left\langle f,\psi_{j,k,m}(x)\right\rangle \tag{5}$$

In this paper, a NonSubsampled Shearlet Transform (NSST) is used. The size of all sub-bands of the image is equal, and its proper feature is being shifted invariant.

2. 3. Singular Value Decomposition A new conversion watermarking method called SVD has been studied in recent years. In the SVD transform, one matrix can be divided into three matrices that are the same size as the original matrix. If *A* is a square image, its corresponding matrix is represented as $A\in R^{n\times n}$, where *R* represents the range of real numbers, so the SVD of matrix *A* is as Equation (6) [40]:

$$A=USV^T=\begin{bmatrix}u_{1,1}&u_{1,2}&\dots&u_{1,N}\\u_{2,1}&u_{2,2}&\dots&u_{2,N}\\\cdot&\cdot&\cdot&\cdot\\\cdot&\cdot&\cdot&\cdot\\\cdot&\cdot&\cdot&\cdot\\u_{N,1}&u_{N,2}&\dots&u_{N,N}\end{bmatrix}\times\begin{bmatrix}\lambda_1&0&\dots&0\\0&\lambda_2&\dots&0\\\cdot&\cdot&\cdot&\cdot\\\cdot&\cdot&\cdot&\cdot\\\cdot&\cdot&\cdot&\cdot\\0&0&\dots&\lambda_N\end{bmatrix}\times\begin{bmatrix}v_{1,1}&v_{1,2}&\dots&v_{1,N}\\v_{2,1}&v_{2,2}&\dots&v_{2,N}\\\cdot&\cdot&\cdot&\cdot\\\cdot&\cdot&\cdot&\cdot\\\cdot&\cdot&\cdot&\cdot\\v_{N,1}&v_{N,2}&\dots&v_{N,N}\end{bmatrix}^T \tag{6}$$

In the above equation $U\in R^{n\times n}$ and each column constitutes the eigenvectors of the matrix AA^T. These special vectors are called left eigenvectors. Also $V\in R^{n\times n}$ represents the matrix that each column represents the eigenvectors of the matrix AA^T. These eigenvectors are called right eigenvectors, and V^T represents the matrix transpose *V*, which is an identity matrix *n x n*. $S\in R^{n\times n}$ is a diagonal matrix with real nonnegative layers on the original diameter. Each element has a single non-descending matrix *A* value. So all of its elements are zero except for the original diameter. λ is a singular value and is defined as follows:

$\lambda_1\ge\lambda_2\ge...\lambda_r\ge\lambda_{r+1}=...=\lambda_N=0$

The SVD is a desirable method for matrix decomposition in which the maximum signal energy is packaged using several coefficients. The use of the SVD in digital image watermarking has many advantages, some of which are as follows [41]:

1. Maximum image energy is obtained by the largest singular value coefficients of the image.
2. Singular image values are very stable. When small damage to the image occurs, its values do not change much, so it is highly resistant to various attacks.
3. Image transparency remains almost constant even after embedding the watermark in singular image values.

2. 4. Whale Optimization Algorithm The scaling factor plays an essential role in watermarking operation. An enormous scale factor value makes the watermark image more robust to attacks. A small scale factor value also makes the watermark image more imperceptible. You have to be smart to choose the right scale factor and balance the watermarking image's resistance and transparency. In this paper, we use Whale Optimization Algorithm (WOA) to select the best scale factor.

The WOA is one of the nature-inspired metaheuristic optimization algorithms [42]. It has shown good performance due to its high convergence speed.

Humpback whales can detect hunting location and circle around them since the optimal position is unknown already in search space. As a result, the WOA algorithm assumes that the current candidate's best answer is the optimal target or the solution is close to it. In the following, other search agents try to update their positions according to the best search factor, such as Equations (7) and (8).

$$\vec{D}=\left|\vec{C}.\vec{X}^*(t)-\vec{X}(t)\right| \tag{7}$$

$$\vec{X}(t+1)=\vec{X}^*(t)-\vec{A}.\vec{D} \tag{8}$$

where t represents the current iteration, $\vec{A}$ and $\vec{C}$ represent the coefficient vectors. X^* indicates the position vector of the best solution to date. $\vec{X}$ represents the current location vector. The $\vec{A}$ and $\vec{C}$ vectors are calculated using Equations (9) and (10):

$$\vec{A}=2\vec{a}.\vec{r}-\vec{a} \tag{9}$$

$$\vec{C}=2.\vec{r} \tag{10}$$

where $\vec{a}$ linearly decreases from 2 to zero during the iterations, and $\vec{r}$ represents a random vector in the interval [0,1].

Humpback whales operate at the exploitation phase using two Shrinking encircling mechanisms and spiral updating position. The contraction loop mechanism is performed by reducing the value of $\vec{a}$ in Equation (9). The distance between the whale at position (X, Y) and the hunting at position (X*, Y*) is first calculated in the spiral position update phase. In the following, a spiral equation is created between the whale position and the hunting position to simulate the spiral motion of humpback whales with Equation (11):

$$\vec{X}(t+1)=\vec{D}'.e^{bl}.\cos(2\pi l)+\vec{X}^*(t) \quad (11)$$

where $\vec{D}'=|\vec{X}^*(t)-\vec{X}(t)|$ and indicates the distance of the *i*th whale to the prey (best solution obtained so far), *b* demonstrates a constant that specifies the shape of the logarithmic spiral, l shows a random number in the range [-1,1].

Humpbacks move around the hunt simultaneously, both in the shape of the shrinking circle and along a spiral-shaped path. We assume that a 50% probability can be used by a contraction loop mechanism or a spiral model to model this synchronous behavior and update the whale's position during optimization. The mathematical model is shown in Equation (12):

$$\vec{X}(t+1)=\begin{cases}\vec{X}^*(t)-\vec{A}.\vec{D} & if\ p<0.5\\ \vec{D}'.e^{bl}.\cos(2\pi l)+\vec{X}^*(t) & if\ p\geq 0.5\end{cases} \quad (12)$$

where p represents a random number in the interval [0,1], vector $\vec{A}$ change-based approach also can be used for hunting search. Humpback whales perform a random search based on each other's position. Therefore, we use random values of $\vec{A}$ greater than one or smaller than minus one to force the search agent to avoid a reference whale. Unlike the extraction phase, we update a search agent's position in the exploration phase based on the randomly selected search agent. This mechanism and $|\vec{A}|>1$ emphasize exploration and allow the WOA algorithm to perform a global search. The mathematical model of this work is given by Equations (13) and (14):

$$\vec{D}=\left|\vec{C}.\vec{X}_{rand}-\vec{X}\right| \quad (13)$$

$$\vec{X}(t+1)=\left|\vec{X}_{rand}-\vec{A}.\vec{D}\right| \quad (14)$$

where $\vec{X}_{rand}$ is the random location vector selected from the current population.

3. PROPOSED METHOD

This paper proposes an invisible watermarking method based on the SVD technique and WOA algorithm in the Non-subsample Shearlet Transform domain. In the suggested algorithm, the host image, the watermark image, and the watermarking image are defined as I, W, and I_w, respectively.

The watermark embedding algorithm in the host image is as follows:

1. Host image I is parsed into three I_R, I_G, and I_B matrices.
2. In matrix I_i ; i=R, G, B, Shearlet transform is executed up to three levels and decomposed into a low-frequency sub-band and some high-frequency sub-bands.
3. In the low-frequency sub-band obtained from the image in step 2, the SVD transform is performed.
4. The dimension of the W watermark image is resized to the sub-dimension of the host image.
5. The watermark image W is split into three W_R, W_G, and W_B matrices.
6. The watermark image is multiplied by the T scale factor. It is aggregated by the matrix of single values (S) obtained from the host image's low-frequency sub-band.
7. The inverse of the SVD transform is obtained by the matrices U and V obtained in step 3 and the matrix S obtained by step 6.
8. The inverse Shearlet transform is executed on the new low-frequency sub-band matrix obtained from step 7. The high-frequency sub-bands obtained from step 2 and the watermarking image I_i ; i=R, G, B is obtained.
9. The three I_R, I_G, I_B matrices obtained from step 8 are merged, and the I_w watermarking is created.
10. The S matrix obtained from level 6 is then stored as a key to retrieving the watermark image.

The watermark extraction algorithm is as follows:

1. Watermarking I_w image is divided into three matrices I_{WR}, $I_{WG,}$ and I_{WB}.
2. In matrix I_W i ; i=R, G, B, Shearlet transform is executed for up to 3 levels and decomposed into a low frequency and some high-frequency sub-bands.
3. In the low-frequency sub-band obtained from step 2, the SVD transform is performed.
4. The matrix S obtained during the watermark's embedding phase (the key to retrieving the watermark image) is called.
5. The inverse of the SVD transform is executed on the U and V matrices obtained from step 3 and the S matrix (watermarking operation key).
6. The inverse Shearlet transform is executed on the low-frequency sub-band matrix obtained from the inverse SVD transform operation obtained from step 5. The rest of the high-frequency sub-bands obtained from step 2 and the watermarking image I_i ; i=R, G, B is obtained.
7. The three I_R, I_G, and I_B matrices obtained from step 6 are merged to create the extracted host image.
8. The S matrix called in step 4 is subtracted from the S matrix obtained in step 3 and then divided into the T scaling factor (alpha), which the WOA algorithm gets its optimal value. (The evaluation function of the WOA algorithm is the Peak Signal to Noise Ratio (PSNR) value between the host and the extracted watermark).

9. The three W_R, W_G, and W_B matrices are merged to create the extracted watermark.

The watermark embedding and extraction algorithm in the host image are shown in Figures 2 and 3, respectively.

4. EVALUATION OF RESULTS

All implementations and results are obtained using MATLAB 2015 software. Two-color images, Airplane and Lena, are used as host images and Peugeot as the watermark image. The used images were afforded from the USC-SIPI database and are standard images for various image processing operations. Figures 4 and 5 show the host images and the watermark image, respectively. The host image size is 128*128 pixels. The watermark is also a 32x32 pixel color image.

In digital watermarking, it is necessary to maintain quality of the original image. Therefore, two criteria of imperceptibility and robustness are needed to evaluate the watermarking and watermark image. These criteria measure the amount of transparency between two images [43]. PSNR is used to measure imperceptibility. The mean square error (MSE) between the two images is measured using Equation (15) [44].

$$MSE(I, I_w) = \frac{1}{MN}\sum_{i=0}^{N-1}\sum_{j=0}^{M-1}(I_1(i,j) - I_2(i,j))^2 \quad (15)$$

M and N are the dimensions of the image, I_1 and I_2 are the primary and the extracted image, respectively.

PSNR is used to estimate the quality of two images. The high PSNR indicates that the two images are very similar [45]. This criterion is expressed in decibel unit (db.) using Equation (16):

$$PSNR(I_1, I_2) = 10 * \log 10 \frac{MAX_I^2}{MSE} \quad (16)$$

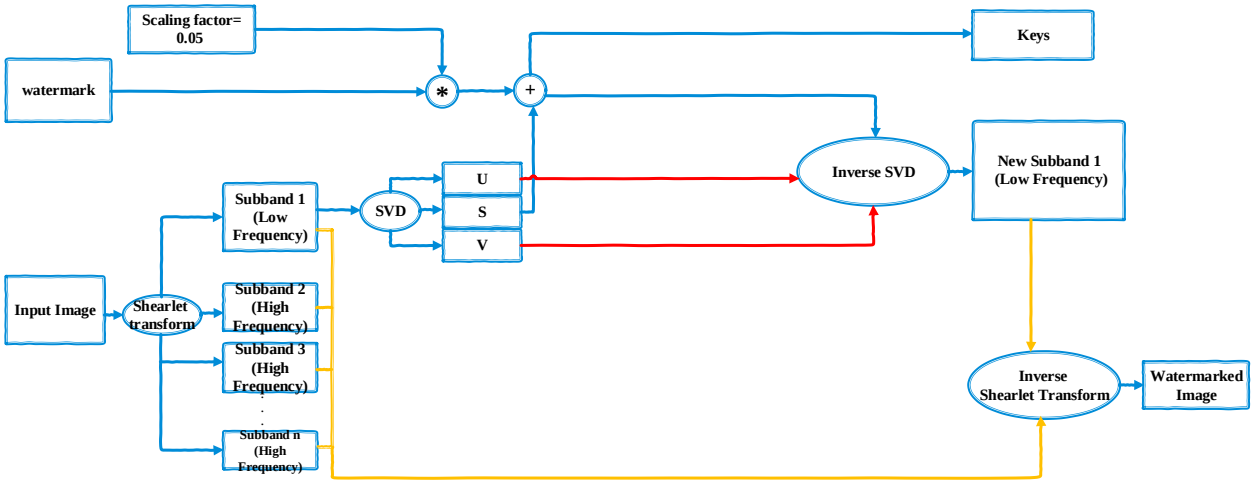

Figure 2. Watermarking embedding algorithm

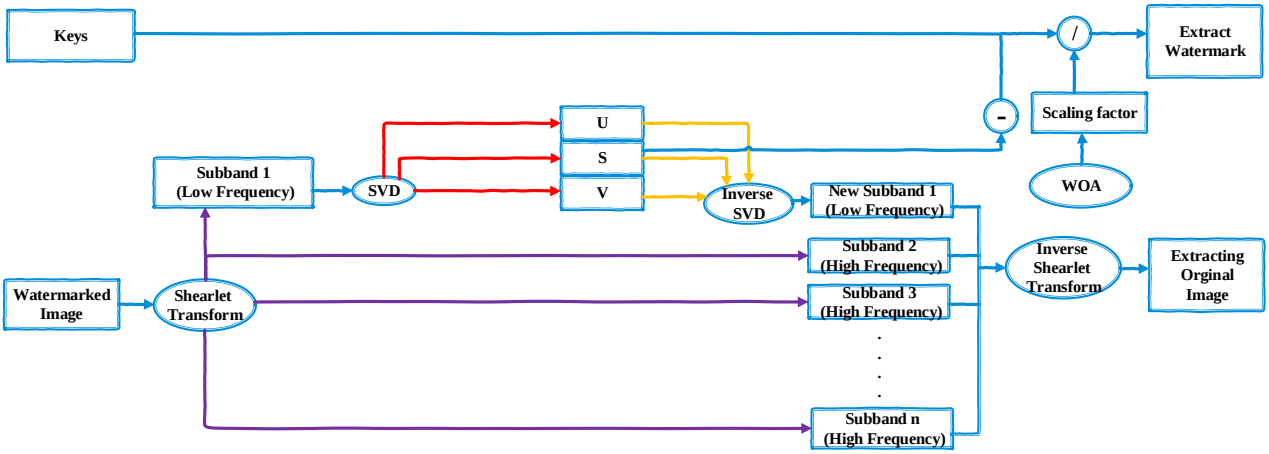

Figure 3. Watermarking extraction algorithm

Figure 4. Images used for the host

Figure 5. Image used for watermarking

MAX_I represents the peak signal in the input image, which is 255 in 8-bit images.

Correlation Coefficient (CRC) can be used to measure the robustness of the extracted watermark. The CRC is used to measure the correlation between the two images. The CRC value ranges from zero to one, calculated using Equation (17) [46].

$$CRC = \frac{\sum_i \sum_j I_1(i,j) I_2(i,j)}{\sqrt{\sum_i \sum_j I_1(i,j)^2 * \sum_i \sum_j I_2(i,j)^2}} \quad (17)$$

I_1 and I_2 are the initial and the extracted image, respectively.

5. EXPERIMENTAL AND COMPARATIVE RESULTS

In this section, results of the proposed method are presented in terms of transparency and robustness according to the experiments. In this method, we have applied Shearlet transform to three levels on the input image. The initial scaling factor value for the watermarking operation was set as 0.05, which is obtained experimentally with relatively good strength and transparency. The WOA algorithm is iterated 100 times.

The proposed method in this paper is compared with similar watermarking techniques using NonSubampled Wavelet Transform (NSWT), NonSubsampled Contourlet Transform (NSCT), DWT_SVD [47], and DST-BSVD [16]. The investigated attacks are as follows: average filter (AF), Gaussian low-pass filter (GP), median filter (MF), Gaussian noise (GN), speckle noise (SN), pepper and salt noise (SP), blurring (BL), motion blur (MB), sharpening (SH), JPEG compression (JPEG), crop (CR), rotation (RO), transition (TR), Vertical flip (FLV), Horizontal flip (FLH).

Comparative results of the extracted watermark transparency based on PSNR criterion and the extracted watermark robustness based on CRC criterion are presented in Table 1. The results of the experiments show that the transparency parameter of the proposed PSNR method is improved on all images compared to the tested methods after AF 3x3, AF 5x5, GP 3x3, GP 5x5, MF 3x3, MF 5x5, RO (5), RO (45), RO (110), FLH, FLV, BL(0.3), BL(0.5), BL(1), MB(15, 45), SH(0.3), SH(0.5), SH(1), JPEG(5), JPEG(20), JPEG(80), JPEG(90), GN(0,0.001), GN(0,0.1), GN(0,0.3), SN(0.001), SN(0.3) and SP(0.3) attacks.

The test results also show that the CRC robustness parameter of the proposed method improved on all images compared to the tested methods after AF 3x3, AF 5x5, GP 3x3 , GP 5x5 , MF 3x3 , MF 5x5 , RO(5) , FLH , FLV , BL(0.3) , BL(0.5) , BL(1) , MB(15,45) , SH(0.3) , SH(0.5) , SH(1) , JPEG(5) , JPEG(20) , JPEG(80) , JPEG(90), GN(0,0.001), GN(0,0.1), GN(0,0.3), SN(0.001) , SN(0.3), and SP(0.001) attacks.

For instance, Lena's watermarking image and the extracted watermark can be seen after applying different image processing attacks in Figure 6.

TABLE 1. Comparison of transparency and robustness of the proposed method with the traditional one

		Airplane Image						Lena Image					
Attacks		NSWT	NSCT	DWT SVD	DST BSVD	NSST WOA	Alpha	NSWT	NSCT	DWT SVD	DST BSVD	NSST WOA	Alpha
No Attack	PSNR	27.5532	27.5422	21.9887	27.6045	27.6082	0.0495	27.5642	27.5374	22.1424	27.6045	27.6722	0.0495
	CRC	0.9976	0.9976	0.9912	0.9976	0.9976		0.9976	0.9976	0.9915	0.9976	0.9976	
AF 3x3	PSNR	-0.0193	20.7062	5.0495	24.4168	24.4186	0.0499	1.3383	21.1577	6.1167	25.9312	25.9561	0.0497
	CRC	0.5612	0.9882	0.7822	0.9949	0.9949		0.617	0.9893	0.8162	0.9964	0.9964	
AF 5x5	PSNR	-6.1806	14.0629	-0.188	20.7052	20.728	0.0506	-5.105	14.5596	0.7797	23.4313	23.4325	0.05
	CRC	0.3434	0.9493	0.6046	0.9881	0.9881		0.3774	0.9544	0.6436	0.9936	0.9936	
GP 3x3	PSNR	9.0892	26.2659	14.7156	27.2263	27.2838	0.0496	10.4572	26.4244	15.9669	27.4432	27.5103	0.0496
	CRC	0.871	0.9967	0.9595	0.9974	0.9974		0.9002	0.9968	0.9691	0.9975	0.9975	

GP 5x5	PSNR	9.034	26.2477	14.6593	27.2223	27.2791	0.0496	10.3999	26.4077	15.9094	27.4415	27.5081	0.0496
	CRC	0.8697	0.9967	0.959	0.9974	0.9974		0.8991	0.9968	0.9687	0.9975	0.9975	
MF 3x3	PSNR	6.854	24.4239	11.3875	27.2733	27.3409	0.0495	8.5258	26.4693	12.1789	27.4907	27.549	0.0495
	CRC	0.8084	0.9949	0.9234	0.9974	0.9974		0.8602	0.9969	0.9353	0.9975	0.9975	
MF 5x5	PSNR	0.927	21.8984	5.5602	26.6743	26.705	0.0496	1.3096	21.9304	5.8633	27.2448	27.2853	0.0495
	CRC	0.5908	0.9909	0.7991	0.997	0.997		0.6147	0.991	0.8083	0.9974	0.9974	
CR (50,50)	PSNR	-0.6669	16.3296	-0.2934	21.0186	21.0333	0.0504	4.6409	21.3338	4.28	17.0051	17.1365	0.0521
	CRC	0.4851	0.968	0.493	0.9889	0.9889		0.7045	0.9897	0.6811	0.9725	0.9725	
RO (5)	PSNR	-1.4583	13.7274	2.6289	15.6693	15.909	0.0533	5.6364	20.0844	8.1568	24.203	24.2561	0.0499
	CRC	0.4235	0.9428	0.6073	0.9634	0.9634		0.7479	0.9862	0.8333	0.9947	0.9947	
RO (45)	PSNR	-9.561	7.6148	-4.1504	16.1511	16.3118	0.0528	-3.7542	13.6737	0.1081	16.1796	16.3986	0.0527
	CRC	0.1379	0.8072	0.2731	0.9669	0.9667		0.343	0.9427	0.5016	0.9671	0.9674	
RO (110)	PSNR	-10.7669	6.2575	-5.1083	10.8244	11.6408	0.0614	-3.8412	13.0419	-0.0082	20.7888	20.8694	0.0505
	CRC	0.1191	0.7586	0.2509	0.8997	0.8989		0.336	0.9343	0.4897	0.9883	0.9885	
TR (5,10)	PSNR	-8.7343	9.8694	-0.3362	5.7629	8.1631	0.0872	-5.6842	12.5935	3.1051	9.187	10.4037	0.0666
	CRC	0.2305	0.88	0.5076	0.7566	0.7565		0.3181	0.9303	0.665	0.8629	0.8629	
TR (10,10)	PSNR	-11.1896	7.3059	-2.7841	3.3138	6.948	0.1153	-8.6026	9.6226	0.2918	6.4978	8.5854	0.0812
	CRC	0.1802	0.8105	0.4145	0.659	0.6589		0.2399	0.875	0.5497	0.7822	0.7823	
TR (10,15)	PSNR	-13.0371	5.364	-4.8295	1.7165	6.3338	0.1442	-10.2198	7.9887	-1.6355	4.9032	7.6904	0.0952
	CRC	0.1513	0.7431	0.348	0.5903	0.5901		0.2063	0.8324	0.4751	0.7231	0.7232	
FLH	PSNR	27.5532	27.5422	21.9887	27.6045	27.68	0.0495	27.5642	27.5374	22.1424	27.6045	27.677	0.0495
	CRC	0.9976	0.9976	0.9912	0.9976	0.9976		0.9976	0.9976	0.9915	0.9976	0.9976	
FLV	PSNR	27.5532	27.5422	21.9887	27.6045	27.6799	0.0495	27.5642	27.5374	22.1424	27.6045	27.68	0.0495
	CRC	0.9976	0.9976	0.9912	0.9976	0.9976		0.9976	0.9976	0.9915	0.9976	0.9976	
BL (0.3)	PSNR	27.2721	27.5422	22.6795	27.6085	27.684	0.0495	27.384	27.5375	22.7695	27.6066	27.6142	0.0495
	CRC	0.9974	0.9976	0.9925	0.9976	0.9976		0.9975	0.9976	0.9927	0.9976	0.9976	
BL (0.5)	PSNR	9.034	26.2477	14.6593	27.2223	27.2796	0.0496	10.3999	26.4077	15.9094	27.4415	27.5043	0.0496
	CRC	0.8697	0.9967	0.959	0.9974	0.9974		0.8991	0.9968	0.9687	0.9975	0.9975	
BL (1)	PSNR	-1.5598	19.1654	3.7335	24.0507	24.0507	0.0499	-0.3246	19.6164	4.795	25.74	25.7613	0.0497
	CRC	0.5009	0.9833	0.7407	0.9945	0.9945		0.5504	0.9849	0.7779	0.9963	0.9963	
MB (15,45)	PSNR	-10.3849	8.3785	-2.8112	13.9633	14.3528	0.0552	-7.7979	10.6649	-0.3996	18.3292	18.386	0.0515
	CRC	0.2275	0.8457	0.4851	0.9472	0.9472		0.2866	0.899	0.5726	0.9796	0.9796	
SH (0.3)	PSNR	27.2895	27.5427	21.548	27.6041	27.6795	0.0495	27.3484	27.5383	21.8401	27.6035	27.6666	0.0495
	CRC	0.9974	0.9976	0.9902	0.9976	0.9976		0.9975	0.9976	0.9909	0.9976	0.9976	
SH (0.5)	PSNR	12.7994	26.7514	12.9629	27.5937	27.6692	0.0495	13.8829	26.729	13.9077	27.5467	27.621	0.0495
	CRC	0.9282	0.9971	0.9284	0.9976	0.9976		0.9431	0.9971	0.942	0.9976	0.9976	
SH (1)	PSNR	2.2872	22.4063	5.302	27.5768	27.6522	0.0495	3.3514	22.6085	6.2613	27.2079	27.2664	0.0496
	CRC	0.5622	0.9919	0.6786	0.9976	0.9976		0.613	0.9923	0.7222	0.9974	0.9974	
JPEG (5)	PSNR	0.1168	17.1102	7.6878	24.2946	24.2964	0.0498	0.6841	18.9329	6.3203	23.9304	23.9319	0.0499
	CRC	0.5055	0.9728	0.8157	0.9948	0.9948		0.5386	0.982	0.7749	0.9943	0.9943	
JPEG (20)	PSNR	5.2668	21.2887	12.0118	27.1215	27.1803	0.0496	7.0401	22.4416	13.4874	27.2512	27.3047	0.0496
	CRC	0.7219	0.9895	0.9151	0.9973	0.9973		0.791	0.992	0.9386	0.9974	0.9974	

JPEG (80)	PSNR	11.4999	25.4888	16.0991	27.5979	27.6697	0.0495	13.3032	26.2067	18.2342	27.608	27.6824	0.0495
	CRC	0.9079	0.9961	0.9652	0.9976	0.9976		0.9372	0.9967	0.9787	0.9976	0.9976	
JPEG (90)	PSNR	14.0842	26.4018	17.9799	27.6153	27.6431	0.0495	15.7238	26.8385	19.7938	27.6108	27.6355	0.0495
	CRC	0.9466	0.9968	0.9774	0.9976	0.9976		0.963	0.9971	0.9853	0.9976	0.9976	
GN (0,0.001)	PSNR	21.6183	27.3805	19.4741	27.6103	27.6748	0.0495	22.6616	27.4792	19.5994	27.5907	27.6624	0.0495
	CRC	0.9904	0.9975	0.9842	0.9976	0.9976		0.9924	0.9975	0.9846	0.9976	0.9976	
GN (0,0.1)	PSNR	-9.893	9.4688	-4.5191	11.4189	12.4969	0.0589	-8.1918	12.9414	-4.0368	15.7908	16.478	0.0526
	CRC	0.1248	0.8672	0.1813	0.9109	0.9181		0.1358	0.9328	0.1761	0.9641	0.9685	
GN (0,0.3)	PSNR	-15.8199	3.3436	-9.2512	4.6152	7.711	0.0952	-12.5428	7.0673	-7.9059	9.3093	11.3599	0.062
	CRC	0.0508	0.6519	0.0654	0.7127	0.7248		0.0607	0.794	0.0576	0.8646	0.8917	
SN (0.001)	PSNR	23.9428	27.4682	20.3124	27.5969	27.6488	0.0495	25.2495	27.5064	21.335	27.5965	27.6447	0.0495
	CRC	0.9944	0.9975	0.987	0.9976	0.9976		0.9959	0.9976	0.9898	0.9976	0.9976	
SN (0.1)	PSNR	-6.8981	12.5193	-1.6489	14.8625	15.2098	0.0541	-3.066	15.8474	1.5968	19.1179	18.6345	0.0513
	CRC	0.2014	0.9274	0.3052	0.9564	0.9569		0.3275	0.9644	0.4785	0.9829	0.9807	
SN (0.3)	PSNR	-14.2862	4.1495	-8.331	5.0541	7.9473	0.0907	-10.0631	8.3206	-5.0202	10.5921	11.4528	0.0618
	CRC	0.0709	0.6865	0.0951	0.73	0.7419		0.1249	0.8358	0.1742	0.8944	0.8944	
SP (0.001)	PSNR	26.4202	27.5591	21.1735	27.6092	27.5918	0.0495	26.1519	27.5369	21.8629	27.587	27.6182	0.0495
	CRC	0.9969	0.9976	0.9893	0.9976	0.9976		0.9967	0.9976	0.991	0.9976	0.9976	
SP (0.1)	PSNR	-5.0013	14.1647	-0.3985	16.0549	16.4447	0.0528	-2.2482	17.8722	1.1564	20.0074	19.8276	0.0508
	CRC	0.2575	0.9487	0.3706	0.9664	0.9682		0.3447	0.9772	0.4384	0.986	0.9854	
SP (0.3)	PSNR	-13.8007	4.9173	-7.5213	6.7054	8.69	0.0803	-10.1943	8.9492	-5.9511	11.3119	12.0809	0.0596
	CRC	0.0729	0.7181	0.1057	0.7902	0.7881		0.1073	0.8531	0.1205	0.908	0.9091	

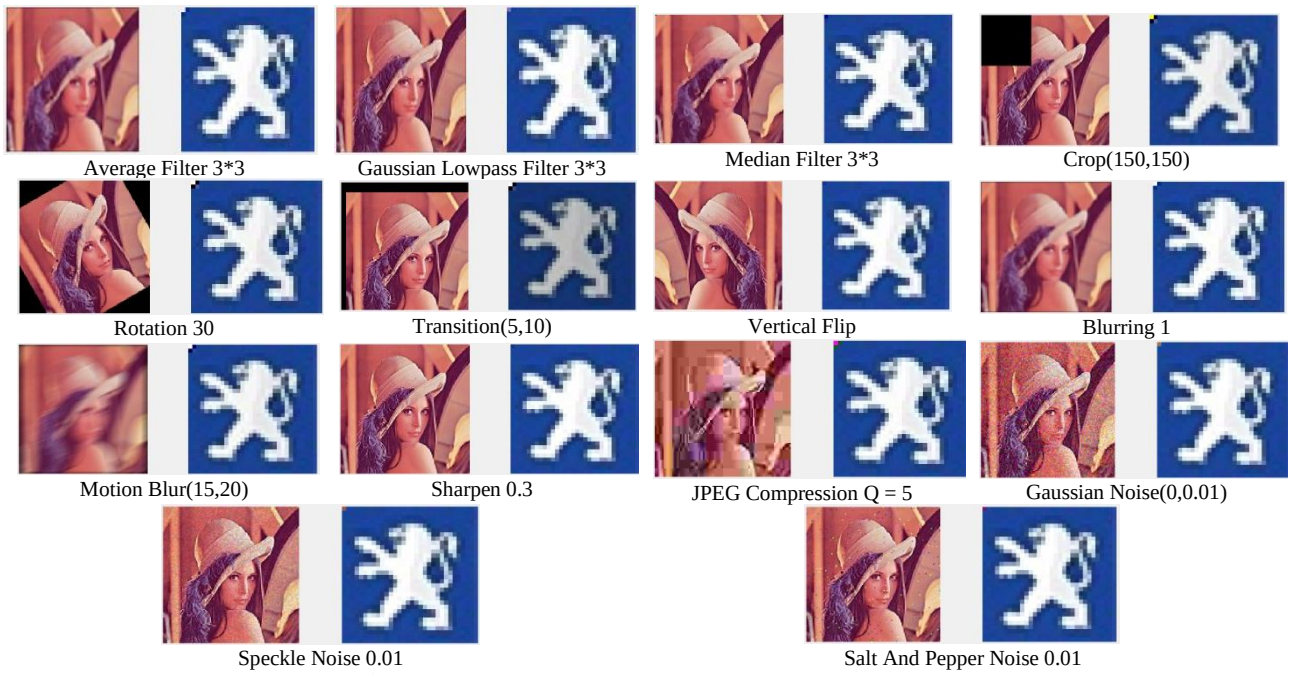

Figure 6. Results of watermarking images (Lena image) and extracted watermark image (Peugeot logo)

We can see the PSNR and the CRC results obtained from the methods tested on different images in Figures 7, 8, 9, and 10, respectively. After various attacks, the result of experiments in the proposed method indicated that we have improved and increased the transparency parameters of PSNR and the CRC robustness parameter over the tested methods. The execution time of the studied algorithms is shown in Table 2.

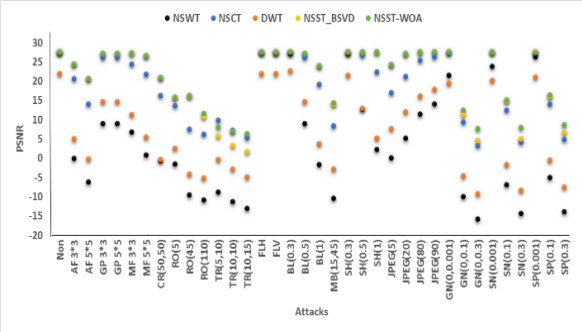

Figure 7. Comparison of the PSNR of the proposed method with the tested methods on the Airplane image

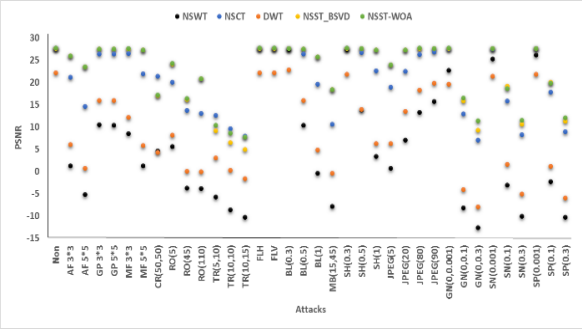

Figure 8. Comparison of the PSNR of the proposed method with the tested methods on the Lena image

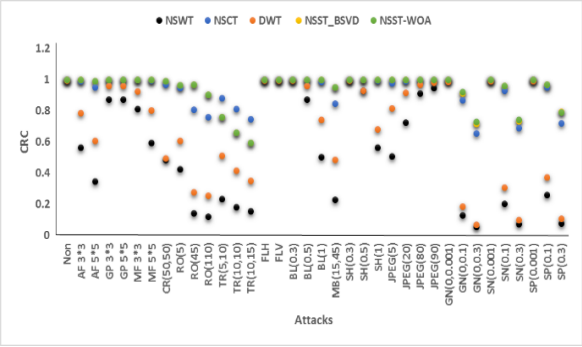

Figure 9. Comparison of the CRC of the proposed method with the tested methods on the Airplane image

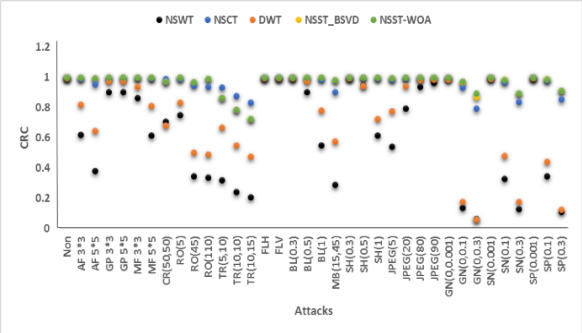

Figure 10. Comparison of the CRC of the proposed method with the tested methods on the Lena image

TABLE 2. Comparison of execution time of the studied algorithms

Algorithm	NSWT	NSCT	DWT SVD	DST BSVD	NSST WOA
Time (second)	0.92	64.23	0.98	2.31	9.90

6. CONCLUSION

In this paper, a new watermarking method using the Shearlet Transform domain coupled with the SVD transform and Whale optimization algorithm is presented with higher transparency and robustness than the comparison methods. Shearlet Transform has more transparency than traditional converts. The SVD transform also increases the robustness of watermarking operations. The whale optimization algorithm is also used to recover the watermark with the least damage in the watermark extraction step. An optimal combination of these methods has resulted in good transparency and resistivity watermarking. The results are extensible in future work and can be tested using other optimization transformations and algorithms.

7. REFERENCES

1. Huang, B.-B. and Tang, S.-X., "A contrast-sensitive visible watermarking scheme", ***IEEE MultiMedia***, Vol. 13, No. 2, (2006), 60-66. DOI: 10.1109/MMUL.2006.23
2. Abdelhakim, A.M., Saleh, H.I. and Nassar, A.M., "A quality guaranteed robust image watermarking optimization with artificial bee colony", ***Expert Systems with Applications***, Vol. 72, No., (2017), 317-326. DOI: 10.1016/j.eswa.2016.10.056
3. Das, C., Panigrahi, S., Sharma, V.K. and Mahapatra, K., "A novel blind robust image watermarking in dct domain using inter-block coefficient correlation", ***AEU-International Journal of Electronics and Communications***, Vol. 68, No. 3, (2014), 244-253. DOI: 10.1016/j.aeue.2013.08.018
4. Wu, X. and Sun, W., "Robust copyright protection scheme for digital images using overlapping dct and svd", ***Applied Soft Computing***, Vol. 13, No. 2, (2013), 1170-1182. DOI: 10.1016/j.asoc.2012.09.028
5. Ali, M., Ahn, C.W. and Siarry, P., "Differential evolution algorithm for the selection of optimal scaling factors in image watermarking", ***Engineering Applications of Artificial Intelligence***, Vol. 31, (2014), 15-26. DOI: 10.1016/j.engappai.2013.07.009
6. Ali, M. and Ahn, C.W., "An optimized watermarking technique based on self-adaptive de in dwt–svd transform domain", ***Signal Processing***, Vol. 94, (2014), 545-556. DOI: 10.1016/j.sigpro.2013.07.024
7. Mishra, A., Agarwal, C., Sharma, A. and Bedi, P., "Optimized gray-scale image watermarking using dwt–svd and firefly algorithm", ***Expert Systems with Applications***, Vol. 41, No. 17, (2014), 7858-7867. DOI: 10.1016/j.eswa.2014.06.011
8. Makbol, N.M., Khoo, B.E. and Rassem, T.H., "Block-based discrete wavelet transform-singular value decomposition image watermarking scheme using human visual system

characteristics", ***IET Image Processing***, Vol. 10, No. 1, (2016), 34-52. DOI: 10.1049/iet-ipr.2014.0965

9. Makbol, N.M. and Khoo, B.E., "A new robust and secure digital image watermarking scheme based on the integer wavelet transform and singular value decomposition", ***Digital Signal Processing***, Vol. 33, (2014), 134-147. DOI: 10.1016/j.dsp.2014.06.012
10. Ansari, I.A., Pant, M. and Ahn, C.W., "Robust and false positive free watermarking in iwt domain using svd and abc", ***Engineering Applications of Artificial Intelligence***, Vol. 49, (2016), 114-125. DOI: 10.1016/j.engappai.2015.12.004
11. Makbol, N.M. and Khoo, B.E., "Robust blind image watermarking scheme based on redundant discrete wavelet transform and singular value decomposition", ***AEU-International Journal of Electronics and Communications***, Vol. 67, No. 2, (2013), 102-112. DOI: 10.1016/j.aeue.2012.06.008
12. Araghi, T.K., Abd Manaf, A. and Araghi, S.K., "A secure blind discrete wavelet transform based watermarking scheme using two-level singular value decomposition", ***Expert Systems with Applications***, Vol. 112, (2018), 208-228. DOI: 10.1016/j.eswa.2018.06.024
13. Araghi, T.K. and Abd Manaf, A., "An enhanced hybrid image watermarking scheme for security of medical and non-medical images based on dwt and 2-d svd", ***Future Generation Computer Systems***, Vol. 101, (2019), 1223-1246. DOI: 10.1016/j.future.2019.07.064
14. Najafi, E. and Loukhaoukha, K., "Hybrid secure and robust image watermarking scheme based on svd and sharp frequency localized contourlet transform", ***Journal of Information Security and Applications***, Vol. 44, (2019), 144-156. DOI: 10.1016/j.jisa.2018.12.002
15. Ali, M., Ahn, C.W., Pant, M. and Siarry, P., "An image watermarking scheme in wavelet domain with optimized compensation of singular value decomposition via artificial bee colony", ***Information Sciences***, Vol. 301, (2015), 44-60. DOI: 10.1016/j.ins.2014.12.042
16. Mardanpour, M. and Chahooki, M.A.Z., "Robust transparent image watermarking with shearlet transform and bidiagonal singular value decomposition", ***AEU-International Journal of Electronics and Communications***, Vol. 70, No. 6, (2016), 790-798. DOI: 10.1016/j.aeue.2016.03.004
17. Fazli, S. and Moeini, M., "A robust image watermarking method based on dwt, dct, and svd using a new technique for correction of main geometric attacks", ***Optik-International Journal for Light and Electron Optics***, Vol. 127, No. 2, (2016), 964-972. DOI: 10.1016/j.ijleo.2015.09.205
18. Vahedi, E., Zoroofi, R.A. and Shiva, M., "Toward a new wavelet-based watermarking approach for color images using bio-inspired optimization principles", ***Digital Signal Processing***, Vol. 22, No. 1, (2012), 153-162. DOI: 10.1016/j.dsp.2011.08.006
19. Maity, S.P., Maity, S., Sil, J. and Delpha, C., "Collusion resilient spread spectrum watermarking in m-band wavelets using ga-fuzzy hybridization", ***Journal of Systems and Software***, Vol. 86, No. 1, (2013), 47-59. DOI: 10.1016/j.jss.2012.06.057
20. Papakostas, G.A., Tsougenis, E. and Koulouriotis, D.E., "Moment-based local image watermarking via genetic optimization", ***Applied Mathematics and Computation***, Vol. 227, (2014), 222-236. DOI: 10.1016/j.amc.2013.11.036
21. Tsai, H.-H., Jhuang, Y.-J. and Lai, Y.-S., "An svd-based image watermarking in wavelet domain using svr and pso", ***Applied Soft Computing***, Vol. 12, No. 8, (2012), 2442-2453. DOI: 10.1016/j.asoc.2012.02.021
22. Tsai, H.-H., Lai, Y.-S. and Lo, S.-C., "A zero-watermark scheme with geometrical invariants using svm and pso against geometrical attacks for image protection", ***Journal of Systems and Software***, Vol. 86, No. 2, (2013), 335-348. DOI: 10.1016/j.jss.2012.08.040
23. Ansari, I.A. and Pant, M., "Multipurpose image watermarking in the domain of dwt based on svd and abc", ***Pattern Recognition Letters***, Vol. 94, (2017), 228-236. DOI: 10.1016/j.patrec.2016.12.010
24. Serdean, C.V., Tomlinson, M., Wade, J. and Ambroze, A.M., "Protecting intellectual rights: Digital watermarking in the wavelet domain", in IEEE Int. Workshop Trends and Recent Achievements in IT. (2002), 16-18.
25. Jian, Z., Shan, L., Jian, J., Wanru, Z. and Shunli, Z., "Extended shearlet-based image watermarking algorithm using selective coefficients in horizontal cone", ***Arabian Journal for Science and Engineering***, Vol. 42, No. 8, (2017), 3597-3607. DOI: 10.1007/s13369-017-2620-1
26. Wang, X.-y., Liu, Y.-n., Xu, H., Wang, A.-l. and Yang, H.-y., "Blind optimum detector for robust image watermarking in nonsubsampled shearlet domain", ***Information Sciences***, Vol. 372, (2016), 634-654. DOI: 10.1016/j.ins.2016.08.076
27. Yahya, A.-N., Jalab, H.A., Wahid, A. and Noor, R.M., "Robust watermarking algorithm for digital images using discrete wavelet and probabilistic neural network", ***Journal of King Saud University-Computer and Information Sciences***, Vol. 27, No. 4, (2015), 393-401. DOI: 10.1016/j.jksuci.2015.02.002
28. Kasmani, S.A. and Naghsh-Nilchi, A.R., "Robust digital image watermarking based on joint dwt-dct", (2009). DOI: 10.4156/jdcta.vol3.issue2.amirgholipour
29. Abdallah, H.A., Hadhoud, M.M., Shaalan, A.A. and El-samie, F.E.A., "Blind wavelet-based image watermarking", ***International Journal of Signal Processing, Image Processing and Pattern Recognition***, Vol. 4, No. 1, (2011). DOI:
30. Zain, J.M. and Clarke, M., "Reversible region of non-interest (roni) watermarking for authentication of dicom images", ***arXiv preprint arXiv:1101.1603***, (2011). DOI: arXiv:1101.1603
31. Banitalebi, A., Nader-Esfahani, S. and Avanaki, A.N., "Robust lsb watermarking optimized for local structural similarity", ***arXiv preprint arXiv:1803.04617***, (2018). DOI: arXiv:1803.04617
32. Wenyin, Z. and Shih, F.Y., "Semi-fragile spatial watermarking based on local binary pattern operators", ***Optics Communications***, Vol. 284, No. 16-17, (2011), 3904-3912. DOI: 10.1016/j.optcom.2011.04.004
33. Ni, Z., Shi, Y.-Q., Ansari, N. and Su, W., "Reversible data hiding", ***IEEE Transactions on circuits and systems for video technology***, Vol. 16, No. 3, (2006), 354-362. DOI: 10.1109/TCSVT.2006.869964
34. Arya, P., Tomar, D.S. and Dubey, D., "A review on different digital watermarking techniques", ***International Journal of Signal Processing, Image Processing and Pattern Recognition***, Vol. 8, No. 10, (2015), 129-136.
35. Kaushik, A.K., "A novel approach for digital watermarking of an image using dft", ***International Journal of Electrical, Electronics & Computer Science Engineering***, Vol. 1, No. 1, (2012), 35-41.
36. Vyas, A., Yu, S. and Paik, J., "Multiscale transforms with application to image processing, Springer, (2018).
37. Labate, D., Lim, W.-Q., Kutyniok, G. and Weiss, G., "Sparse multidimensional representation using shearlets", in Wavelets XI, International Society for Optics and Photonics. Vol. 5914, No. Issue, (2005), 59140U. DOI: 10.1117/12.613494
38. Guo, K. and Labate, D., "Optimally sparse multidimensional representation using shearlets", ***SIAM Journal on Mathematical Analysis***, Vol. 39, No. 1, (2007), 298-318. DOI: 10.1137/060649781
39. Favorskaya, M.N., Jain, L.C. and Savchina, E.I., Perceptually tuned watermarking using non-subsampled shearlet transform, in

Computer vision in control systems-4. 2018, Springer.41-69. DOI: 10.1007/978-3-319-67994-5_3

40. Vaidya, P. and PVSSR, C.M., "A robust semi-blind watermarking for color images based on multiple decompositions", ***Multimedia Tools and Applications***, Vol. 76, No. 24, (2017), 25623-25656. DOI: 10.1007/s11042-017-4532-1.
41. Vali, M.H., Aghagolzadeh, A. and Baleghi, Y., "Optimized watermarking technique using self-adaptive differential evolution based on redundant discrete wavelet transform and singular value decomposition", ***Expert Systems with Applications***, Vol. 114, (2018), 296-312. DOI: 10.1016/j.eswa.2018.07.004
42. Mirjalili, S. and Lewis, A., "The whale optimization algorithm", ***Advances in Engineering Software***, Vol. 95, (2016), 51-67. DOI: 10.1016/j.advengsoft.2016.01.008
43. Wang, Z., Bovik, A.C., Sheikh, H.R. and Simoncelli, E.P., "Image quality assessment: From error visibility to structural similarity", ***IEEE Transactions on Image Processing***, Vol. 13, No. 4, (2004), 600-612. DOI: 10.1109/TIP.2003.819861
44. Mousavi, S.M., Naghsh, A. and Abu-Bakar, S., "Watermarking techniques used in medical images: A survey", ***Journal of Digital Imaging***, Vol. 27, No. 6, (2014), 714-729. DOI: 10.1007/s10278-014-9700-5
45. Heylen, K. and Dams, T., "An image watermark tutorial tool using matlab", in Mathematics of Data/Image Pattern Recognition, Compression, and Encryption with Applications XI, International Society for Optics and Photonics. Vol. 7075, (2008), 70750D. DOI: 10.1117/12.793308
46. Jabade, V.S. and Gengaje, D.S.R., "Literature review of wavelet based digital image watermarking techniques", ***International Journal of Computer Applications***, Vol. 31, No. 1, (2011), 28-35.
47. Arora, S.M., "A dwt-svd based robust digital watermarking for digital images", ***Procedia Computer Science***, Vol. 132, (2018), 1441-1448. DOI: 10.1016/j.procs.2018.05.076

Persian Abstract

چکیده

نهان نگاری برای پنهان کردن یا اضافه کردن داده یا فایلی در فایل دیگر, به طوری که فقط افراد آگاه با ابزار لازم بتوانند به آن دست یابند و همچنین یکی از راه‌های حفاظت از داده‌های چندرسانه‌ای در برابر کپی برداری‌های غیرقانونی و توزیع غیرقانونی آن ها است. در روش های قبلی نهان نگاری, تصاویر دیجیتال بیشتر از روش هایی مانند تبدیلات فوریه و تبدیلات موجک و روش‌های ریاضی و آماری دیگری استفاده می‌شد. تبدیل قیچک که نوع خاص و نسبتاً جدیدی می باشد می تواند برای نهان نگاری در تصاویر دیجیتال نیز مورد استفاده قرار گیرد. این روش به دلیل ویژگی‌های خاص خود می‌تواند باعث افزایش اثر و بهره وری در کاربردهایی مانند نهان نگاری تصاویر مورد استفاده قرار گیرد. در این مقاله بر خلاف روش‌های قدیمی برای افزایش شفافیت و مقاومت تصویر نهان نگاری شده, نهان نگاره در زیر باند فرکانس پایین تصویر میزبان جاسازی شده است و از تبدیل SVD به همراه الگوریتم بهینه سازی WOA برای به دست آوردن بهترین فاکتور مقیاس آلفا در مرحله استخراج نهان نگاره پس از اعمال انواع حملات مختلف پردازش تصویری استفاده شده است. همچنین روش مورد مطالعه بر روی تصاویر میزبان و تصاویر نهان نگاره رنگی اجرا شده است. نتایج آزمایشات مختلف نشان دهنده این می‌باشد که روش جدید ارایه شده در این مقاله نسبت به روش‌های نهان نگاری مورد مقایسه از لحاظ مقاومت و شفافیت دارای نتایج بهتری در مقابل اکثر حملات پردازش تصویری می باشد.